Chemistry & Biology
Article

# Proposed Arrangement of Proteins Forming a Bacterial Type II Polyketide Synthase

Gaetano Castaldo,[1,6] Jurica Zucko,[2,3,6] Sibylle Heidelberger,[1] Dušica Vujaklija,[4] Daslav Hranueli,[2] John Cullum,[3] Pakorn Wattana-Amorn,[5] Matthew P. Crump,[5] John Crosby,[5] and Paul F. Long[1,*]
[1]School of Pharmacy, University of London, 29-39 Brunswick Square, Bloomsbury, London WC1N 1AX, UK
[2]Faculty of Food Technology and Biotechnology, University of Zagreb, Pierottijeva 6, 10000 Zagreb, Croatia
[3]Department of Genetics, University of Kaiserslautern, Postfach 3049, 67653 Kaiserslautern, Germany
[4]Department of Molecular Biology, Ruđer Bošković Institute, PO Box 180, 10002 Zagreb, Croatia
[5]School of Chemistry, University of Bristol, Cantock's Close, Bristol BS8 1TS, UK
[6]These authors contributed equally to this work
*Correspondence: paul.long@pharmacy.ac.uk
DOI 10.1016/j.chembiol.2008.09.010

## SUMMARY

**Aklanonic acid is synthesized by a type II polyketide synthase (PKS) composed of eight protein subunits. The network of protein interactions within this complex was investigated using a yeast two-hybrid system, by coaffinity chromatography and by two different computer-aided protein docking simulations. Results suggest that the ketosynthase (KS) α and β subunits interact with each other, and that the KSα subunit also probably interacts with a malonyl-CoA:ACP acyltransferase (DpsD), forming a putative minimal synthase. We speculate that DpsD may physically inhibit the priming reaction, allowing the choice of propionate rather than acetate as the starter unit. We also suggest a structural role for the cyclase (DpsY) in maintaining the overall structural integrity of the complex.**

## INTRODUCTION

The diversity of biological processes is due to dynamic associations between cellular components, including noncovalent protein-protein and protein-ligand interactions (Parrish et al., 2006). For a number of metabolic pathways, several enzymes that catalyze sequential reactions often associate noncovalently to form a multienzyme complex. Such complexes afford increased reaction rates and protect labile intermediates from decomposition by channeling intermediates directly from one active site to another. Studies on enzyme complex formation and substrate channeling are essential for a better understanding of metabolism. To achieve this, we need to know the reactive groups involved at the active sites of the enzymes, the amino acids involved in surface binding sites, the specific order in which the large protein complexes are assembled, and the overall topology of the complex. Polyketides are a large and structurally diverse group of natural products that display an impressive range of biological activities of major economic importance to the pharmaceutical and agrochemical industries. These compounds are synthesized by large multienzyme systems called polyketide synthases (PKSs) that catalyze the sequential decarboxylative condensation between short chain coenzyme A (CoA)-derived carboxylic acids by a mechanism analogous to fatty acid biosynthesis. The growing carbon chain backbone then undergoes regio- and stereoselective modification to give the final natural product.

Type II PKSs consist of several discrete, monofunctional proteins that form a dissociable complex, usually leading to the biosynthesis of aromatic polyketides (Hertweck et al., 2007). A minimal type II PKS is formed on association of a ketosynthase (KS), termed KSα, a KS homolog lacking the active site cysteine, often referred to as the chain length factor (CLF) or KSβ, and an acyl carrier protein (ACP). This minimal system controls starter unit selection, chain length, and the first cyclization of the nascent polyketide chain. A fourth enzyme, malonyl-CoA:ACP acyltransferase (MCAT), may be required for substrate loading in vivo (Revill et al., 1995; Summers et al., 1995), although the demonstration of an inherent malonyl transferase activity of the type II ACP indicates that MCAT may not be needed in vitro (Hitchman et al., 1998; Matharu et al., 1998). Additional enzymes, such as ketoreductase (KR), cyclase (CYC), and aromatase (ARO), associate with the minimal complex to generate aromatic natural products (McDaniel et al., 1995; Kramer et al., 1997; Funa et al., 1999; Petkovic et al., 1999). There is currently very little detailed information about the three-dimensional (3D) organization of type II PKS complexes, a factor that undoubtedly limits the rational design of novel polyketides in these systems. Much more information is available on individual protein structures associated with type II PKSs. The X-ray structure of the heterodimeric KS/CLF from *Streptomyces coelicolor* has been solved and the cavity that determines chain length identified (Keatinge-Clay et al., 2003). A number of solution structures for PKS ACPs are available (Crump et al., 1997; Findlow et al., 2003; Li et al., 2003), although, as yet, the exact nature of the protein-protein interactions between the carrier protein and the KS/CLF heterodimer that allow the formation of an active minimal complex remain to be identified. Several auxiliary enzymes that may interact either with the minimal complex or the ACP component of the complex have also been structurally characterized. These include the KR from *S. coelicolor* (Hadfield et al., 2004; Korman et al., 2004), the methyltransferase from *Streptomyces peucetius* (Jansson et al., 2004), and the CYC from *Streptomyces nogalater* (Sultana et al., 2004), *Streptomyces glaucescens* (Thompson et al., 2004), and *Streptomyces galilaeus* (Sultana et al., 2004). The CYC may be particularly important for

 

**Table 1. Matrix of Possible Protein-Protein Interactions for the Entire Daunorubicin/Doxorubicin-Producing PKS Measured Using a Y2H Assay**

| | Bait | | | | | | | |
|---|---|---|---|---|---|---|---|---|
| Prey | A (KSα) | B (KSβ) | C (KSIII) | D (MAT) | G (ACP) | E (KR) | F (ARO) | Y (CYC) |
| A (KSα) | AA++ | AB++ | AC | AD | AG+ | AE | AF+ | AY+ |
| B (KSβ) | BA | BB | BC | BD+ | BG+ | BE+ | BF+ | BY |
| C (KSIII) | CA | CB | CC | CD | CG+ | CE+ | CF+ | CY+ |
| D (MAT) | DA++ | DB+ | DC | DD | DG+ | DE++ | DF+ | DY+ |
| G (ACP) | GA | GB | GC | GD | GG | GE+ | GF | GY+ |
| E (KR) | EA | EB | EC | ED+ | EG+ | EE | EF+ | EY+ |
| F (ARO) | FA+ | FB | FC | FD+ | FG+ | FE+ | FF+ | FY+ |
| Y (CYC) | YA++ | YB++ | YC+ | YD++ | YG | YE++ | YF | YY++ |

ACP, acyl carrier protein; ARO, aromatase; CYC, cyclase; KR, ketoreductase; KS, ketosynthase; MCAT, malonyl-CoA:ACP acyltransferase. "++" indicates strong interactions revealed by nutritional selection, while "+" indicates weak interactions revealed by *LacZ* β-galactosidase assay.

the stability of the overall complex, as its addition eliminates the production of shorter polyketides as well as increasing the turnover of the complex (Yu et al., 1998).

Daunorubicin (DNR) and the C-14 hydroxylated derivative, doxorubicin, are among the most widely used antitumor anthracyclines (Minotti et al., 2004). Both anthracyclines are produced by *S. peucetius* through a pathway involving a type II PKS (Keatinge-Clay et al., 2004). This PKS catalyzes the condensation between a propionyl-CoA starter unit and nine malonyl-CoA extender units, producing a 21 carbon decaketide. Aldol condensation followed by C-12 oxidation of the decaketide leads to the formation of the first enzyme-free intermediate, aklanonic acid. The gene cluster encoding DNR biosynthesis consists of eight genes, designated *dpsA*, *-B*, *-C*, *-D*, *-G*, *-E*, *-F*, and *-Y* (Grimm et al., 1994). Genes *dpsA* and *-B* encode the KS and CLF enzymes, while the ACP is encoded by *dpsG*, unusually positioned 6.8 kb upstream of the position seen in other type II PKSs. This PKS is also unusual in the choice of a propionate rather than an acetate starter unit (Rajgarhia and Strohl, 1997), with the enzymes encoded by *dpsC* and *-D* playing a crucial role in the specification of this starter unit (Bao et al., 1999a, 1999b). The enzyme encoded by *dpsC* is a homolog of the β-ketoacyl: ACP synthase III (KASIII) responsible for the condensation between the starter unit and the first extender unit, while *dpsD* encodes a proposed MCAT (Rajgarhia and Strohl, 1997). The genes *dpsC* and *-D* are rare, and equivalent enzymes have only been described in this and other type II PKS clusters that utilize nonacetate starters (Bibb et al., 1994; Piel et al., 2000; Raty et al., 2002). Their role in starter unit selection is not, however, entirely clear, as deleting *dpsC* but not *dpsD* shifted starter unit selection from propionate to predominantly acetate (Rajgarhia and Strohl, 1997), suggesting that *dpsC* and not *dpsD* contributes to, but does not dictate, starter unit selection. The *dpsE* gene product is a KR, with *dpsF* coding for an ARO (Meurer et al., 1997). Although initial studies failed to identify the function of *dpsY* (Lomovskaya et al., 1998), it was known to be essential for the production of DNR in *S. peucetius*, as its deletion leads to the formation of aberrant cyclization products. Its function as a CYC was later confirmed (Wohlert et al., 2001). To date, few of the type II DNR PKS enzymes have been expressed and purified; none have been structurally characterized. In this article, we extend our initial studies (Castaldo et al., 2005) to obtain further information on the in vivo protein-protein interactions involved in the biosynthesis of aklanonic acid.

## RESULTS AND DISCUSSION

### Investigating Protein-Protein Interactions Using a Yeast Two-Hybrid System

To investigate interactions between proteins forming the minimal aklanonic acid-producing PKS (Grimm et al., 1994; Hutchinson and Colombo, 1999), the genes encoding the KS subunits (α, *dpsA*; β, *dpsB*), the ACP (*dpsG*), the KASIII (*dpsC*), and MCAT (*dpsD*) were cloned and assayed as both prey and bait using a matrix of all possible protein interactions (Table 1). All potential interactions were tested independently three times along with the relative controls. Strong interactions were assessed by nutritional selection using *ADE2* and *HIS3* markers. The results from these assays (Table 1) suggest that DpsA (KSα) interacted with DpsB (KSβ or CLF). Such an interaction between the KS subunits has been described for many complexes. It has also been known for some time that, if the equivalent subunits from other type II PKS systems are expressed and purified, they coelute, suggesting strong, noncovalent interactions (Carreras and Khosla, 1998; Matharu et al., 1998). These interactions can be identified from the crystal structure of the actinorhodin KS/CLF heterodimer (Keatinge-Clay et al., 2004). The assays also suggest that KSα (DpsA) interacts strongly with itself, in contrast to the actinorhodin KSα, which is monomeric (Keatinge-Clay et al., 2004). Structural studies of the actinorhodin KSα-KSβ have demonstrated that these two proteins form an amphipathic tunnel, with polyketide synthesis at the heterodimer interface (Keatinge-Clay et al., 2004). This structure is thought to predict overall chain length as well as partially specifying correct first-ring cyclization. The aklanonic acid-producing KSα-KSβ proteins also show strong interactions and, by analogy with the actinorhodin system, may dictate chain length and correct cyclization in a similar fashion. It has been suggested that the actinorhodin KSβ acts as a malonyl-CoA decarboxylase, thereby generating the acetyl-ACP starter for this biosynthetic pathway (Bisang et al., 1999). This has not been unanimously accepted, with the KSα implicated as the alternative source of the decarboxylase activity (Dreier and Khosla, 2000), nor has such an activity been identified in KSβ (DpsB). It is known that acetyl-CoA can act as a starter unit in

anthracycline biosynthesis, suggesting that decarboxylation by either of the KS subunits would be unnecessary (Rajgarhia and Strohl, 1997). Decarboxylation has not been ruled out, however, and the weak interactions between ACP and both of the KS subunits suggest that this may still be a possibility.

Interestingly, the nutritional selection assays also revealed a strong interaction between KS$\alpha$ (DpsA) and the MCAT, DpsD, but its role in aklanonic acid biosynthesis is not clear, as deletion of *dpsD* from the gene set does not affect compound production (Grimm et al., 1994). In addition, initial experiments involving heterologous expression of all of the genes involved in aklanonic acid production, but excluding *dpsC* and *dpsD*, seemed to result in synthesis of the correct tricyclic 21 carbon intermediate (Rajgarhia and Strohl, 1997). However, the polyketide SEK43 was produced in subsequent in vitro studies, indicating the use of acetyl, and not propionyl-CoA, to form this aberrant cyclized product (Meurer et al., 1997). The anthracycline, feudomycin D, could also be isolated from the *dpsC* and *dpsD* mutant (Rajgarhia and Strohl, 1997). This anthracycline is formed via desmethylaklanonic acid, again an acetate-initiated polyketide, with miscyclization to SEK43 prevented by the presence of additional cyclases. DNR is also produced in this system, but only at 40% of control levels. The correct propionate starter could only be ensured if *dpsC* (though not necessarily in tandem with *dpsD*) was present, confirming the suggestion that the *dpsC* gene product specifies propionyl starter unit selection (Grimm et al., 1994; Rajgarhia et al., 2001). It has been suggested that KASIII (DpsC), along with KS$\alpha$ (DpsA) and KS$\beta$ (DpsB), are together responsible for this process, so it is surprising that KASIII (DpsC) does not appear to interact strongly with the KS subunits, nor does it interact with MCAT (DpsD), suggesting that these are not a tandem pair of enzymes. The MCAT (DpsD) does not appear to select the CoA-derived polyketide starter, and its absence in vivo still leads to the production of aklanonic acid. In vitro, however, extracts containing all of the PKS genes, except MCAT (DpsD), failed to produce any polyketide products irrespective of whether propionyl- or acetyl-CoA were provided to initiate the biosynthesis (Rajgarhia et al., 2001), suggesting a structural role within the complex. This has also been observed for other type II systems that contain an MCAT (DpsD) homolog (Tang et al., 2004), suggesting instability in the PKS complex that may be compensated for in vivo by other cellular components. Indeed, crosstalk between the *S. coelicolor* FAS malonyl transferase and the actinorhodin PKS complex has previously been suggested (Summers et al., 1995; Raty et al., 2002). Alternatively, MCAT (DpsD) may act as an acyl-ACP thioesterase, which selectively hydrolyzes acetyl groups, thereby favoring propionyl starter selection. This activity has been described for ZhuC, a homologous enyzyme to MCAT (DpsD), which acts as part of the initiation module from the R1128-producing PKS (Tang et al., 2003).

No strong interactions between the *dpsG* gene product (the ACP), and either the KS subunits (DpsA and B), or KASIII (DpsC) or MCAT (DpsD), could be detected, suggesting that interactions between the ACP and these components of the complex are weak or transient. No phosphopantetheinyl (PPT) transferase (PPTase) has yet been identified that is involved in secondary metabolism in *Saccharomyces cerevisiae* (Wattanachaisaereekul et al., 2008). It has been demonstrated that heterologous expression of the 6-methylsalicylic acid synthase from *Penicillium patulum* in *S. cerevisiae* does require coexpression of an exogenous PPTase to convert apo-ACP to its holo form (Kealey et al., 1998; Wattanachaisaereekul et al., 2008). PPT phosphate may well be a major binding-energy contributor, so it is feasible that no strong interactions between the ACP (DpsG) and the other domains were observed because the ACP (DpsG) was in the apo form when expressed in *S. cerevisiae* for the yeast two-hybrid (Y2H) assay. For this reason, and in order to investigate potentially weaker interactions between the proteins of the minimal DNR PKS, *LacZ* assays were performed on combinations where no interactions could be observed by nutritional selection (shown in Table 1). When no interactions were detected either by nutritional selection or by *lacZ* assay, Western blots confirmed protein expression in the yeast heterologous host (data not shown). Using the *lacZ* assay, weak interactions were observed between the ACP (DpsG) and both of the KS subunits, as well as the KASIII homolog (DpsC) and the MCAT (DpsD). A homodimeric interaction between two ACPs was not observed. Such an interaction has been described for several type II PKS ACPs (Hitchman et al., 1998; Matharu et al., 1998; Florova et al., 2002), an interaction that facilitates the inter-ACP transfer of malonate. It is possible that, in the aklanonic acid-producing PKS, this acyl transfer is performed by another component of the complex, possibly MCAT (DpsD). ACPs are known to be essential for polyketide production in a number of type II minimal systems (McDaniel et al., 1995; Matharu et al., 1998), and it has been shown that the levels of ACP may be a limiting factor in the production of these secondary metabolites (Decker et al., 1994; Matharu et al., 1998). A model for the *S. coelicolor* actinorhodin minimal PKS complex has been described where the ACP dissociates from the KS/CLF after each round of condensation (Dreier and Khosla, 2000). This model would also be consistent with the observation that the ACP interacts weakly with the other components of the minimal complex. The weak interaction between the ACP and KASIII (DpsC) supports the hypothesis that the KASIII homolog acts in the priming reaction catalyzing the condensation of the starter unit, propionyl-CoA, to a malonyl-CoA extender unit with the product transferred to the 4′-phosphopantetheine thiol of the ACP. No homodimeric interactions involving KASIII (DpsC) were observed, as supported by previous studies (Bao et al., 1999a, 1999b), although this appears to be a unique feature in the aklanonic acid-producing PKS, since other KASIII-like proteins—for example, the FabH of *Escherichia coli* (Qin et al., 2001; Qiu et al., 2001) and ZhuH in R1128 biosynthesis (Pan et al., 2002)—show a homodimeric structure.

Finally, the proteins involved in auxiliary processing of the growing polyketide carbon chain, the KR (DpsE), the ARO (DpsF), and the CYC (DpsY) were investigated. As before, initial screening was performed by nutritional selection to indicate the strongest interactions, while weaker interactions were highlighted using the *LacZ* assay. Results, shown in Table 1, revealed that the CYC (DpsY) interacts strongly with the two subunits of the KS (DpsA and DpsB), with the MCAT (DpsD), and with the KR (DpsE). The CYC also interacts strongly with itself, suggesting either a dimeric or tetrameric arrangement, quaternary structures that have also been observed for the tetracenomycin F2 CYC from *S. glaucescens* (Thompson et al., 2004) and for SnoaL, the enzyme catalyzing the last cyclization step in *S. nogalater* (Beinker et al., 2006). A stronger interaction was also observed

between MCAT (DpsD) and the KR (DpsE). For DpsE, there appears to be no indication of a dimeric form, which has been described for the actinorhodin KR (Hadfield et al., 2004; Korman et al., 2004). Weak interactions between all of the enzymes tested were observed, with the exception of KSα (DpsA) with KR (DpsE), and KR (DpsE) with itself.

As with all techniques, the interpretation of the results must take into account the limitations of the methods used, and the Y2H approach has a number of well-documented disadvantages. False-positive interactions are possible through autoactivation of the bait fusion. False-negative interactions may also arise through incorrect folding of either the bait or prey chimeric proteins. Many proteins also require posttranslational modifications in order to attain the correct structure and full biological activity, and the Y2H assay may fail to detect proteins whose interactions depend on such modifications. The necessity for phosophopantetheinylation of the ACP in order to generate the active form is well documented (Mootz et al., 2001), although covalent modifications have also been identified for other type II PKS enzymes. Some are subjected to proteolytic processing, while others show a combination of truncation and covalent addition (Gramajo et al., 1991; Hesketh et al., 2002). The Y2H system may also be unsuitable for the detection of interactions with membrane proteins, which may be improperly folded due to exposed, highly hydrophobic patches. This may be a particular problem for the KS, as this enzyme, which is central to the PKS minimal complex, may be membrane associated (Gramajo et al., 1991).

## Investigating Protein-Protein Interactions Using Tandem Affinity Purification

From the Y2H results, KSα (DpsA) appeared to be central to the formation of a ''minimal'' PKS, which we speculate to be a homodimer composed of a head-to-tail arrangement of KSα (DpsA), KSβ (DpsB), and MCAT (DpsD). Tandem affinity purification (TAP) (Rigaut et al., 1999) was used to investigate this association further, with the TAP tag fused at the N terminus of KSα (DpsA). This technique allows purification of protein complexes under native conditions by using two different affinity purification steps. Expression of the minimal PKS with the hybrid protein TAP tag-DpsA was performed under the control of the strong constitutive promoter *ermE*p* (Carreras and Khosla, 1998) using the heterologous host *S. coelicolor* A3(2). Transcription of *dpsA*, *dpsB*, *dpsC*, *dpsD*, and *dpsG* were detected by RT-PCR. The presence of hybrid protein TAP tag-DpsA was detected by immunoblotting using IgG antibody that binds the ProtA epitope located at the N terminus of the TAP tag. Subsequent analysis of the protein eluates collected at the end of the purification step by SDS-PAGE revealed the presence of only KSα (DpsA) and KSβ (DpsB), which was confirmed by mass spectrometry. Proteins corresponding to KASIII (DpsC), MCAT (DpsD), or the ACP (DpsG) could not be detected by SDS-PAGE followed by staining with Coomassie brilliant blue (a one-dimensional [1D] SDS-PAGE gel is shown in the Supplemental Data available online—see Figure S1).

Strong interaction between KSα (DpsA) and KSβ (DpsB) was not unexpected, since similar interactions had been predicted from the X-ray crystal structure of KSα/KSβ from the actinorhodin-producing PKS (Keatinge-Clay et al., 2004) and by copurification of these proteins by gel chromatography as an $\alpha_2\beta_2$ heterotetramer (Carreras and Khosla, 1998). Comparison with the crystal structure of the actinorhodin KSα/KSβ complex would suggest that the N terminus of KSα (DpsA) is sufficiently exposed and not involved in crucial interactions with KSβ (DpsB). However, the presence of the TAP tag in this region of the protein might have impaired the interaction with the other ''minimal'' components, such as MCAT (DpsD). Failure to recover KASIII (DpsC) and the ACP (DpsG) might have been expected, since these proteins were found to form only weak interactions with the minimal PKS by the *lacZ* assay in the Y2H screen. This has also been suggested by the proposed mechanism of action of KASIII in type II fatty acid biosynthesis (Jackowski et al., 1989) and the ACP in the biosynthesis of thiolactomycin by *E. coli* (White et al., 2005).

## Investigating Protein-Protein Interactions by Computer Simulation

ClusPro (Comeau et al., 2003) is a fully automated, Web-based program for docking protein structures. It is designed as a multistage protocol, which first performs rigid body searches using ZDOCK (Chen et al., 2003). ZDOCK uses fast Fourier transform to search all possible binding modes for the proteins. Its scoring functions combine shape complementarity, desolvation energy, and electrostatics in its calculations. Docked structures are then filtered using distance-dependent electrostatics and an empirical potential representing desolvation. The 2000 conformations retained after filtering are clustered based on pairwise root-mean-square deviation (rmsd), which is the measure of the average distance between the backbones of the superimposed proteins. The representative conformations from the 30 largest clusters are selected and refined using a brief CHARMm minimization (CHARMm is a program within ClusPro for macromolecular energy, minimization, and dynamics calculations). In our docking simulations, the first 10 cluster representatives were retained.

As second docking simulations, PatchDock (Schneidman-Duhovny et al., 2005), in conjunction with FireDock (Mashiach et al., 2008), were used to evaluate the results obtained by ZDOCK. PatchDock (Duhovny et al., 2002) is a geometry-based molecular docking algorithm. The PatchDock algorithm divides the Connolly dot surface representation of the molecules into concave, convex, and flat patches. Complementary patches are then matched in order to generate candidate transformations. Each candidate transformation is further evaluated by a scoring function that considers both geometric fit and atomic desolvation. FireDock (Andrusier et al., 2007) is a method for the refinement and rescoring of the rigid-body docking solutions. Each candidate generated by the rigid-body docking method was refined using a restricted interface side chain rearrangement and by soft, rigid-body optimization. Refined candidates are then ranked by the binding score, which includes atomic contact energy, softened van der Waals interactions, partial electrostatics, and additional estimations of the binding free energy. The output is a ranked list of all the input solutions. For docking simulations, PatchDock was used with default settings, and the first 100 solutions were refined using Firedock. The top 10 results from FireDock were retained.

The use of docking algorithms to investigate protein interactions requires knowledge of the tertiary structure of the putative

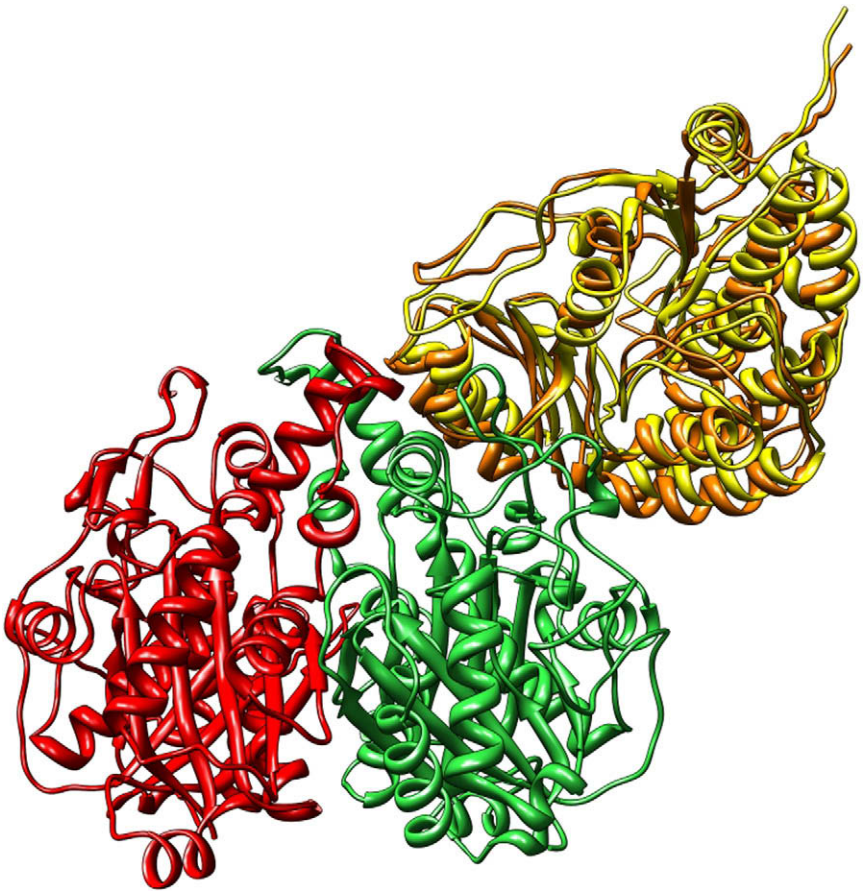

**Figure 1. Computational Docking Simulating the Protein-Protein Interactions between DpsAB and DpsD**

The DpsA (green)/DpsB (red) interaction matches the predicted 2.0 Å X-ray crystal structure of the KS subunits from the actinorhodin-producing PKS. The simulation also supports the Y2H (Table 1) results where a strong interactions between DpsA/DpsB and DpsA/DpsD were observed. These results also suggest that the failure to pull down an intact DpsAB/DpsD complex could be due to the design of the coaffinity chromatography, as discussed in the main text. DpsD is shown in yellow.

interacting proteins. However, the number of structurally characterized proteins is extremely low compared with the annotated primary structure of proteins present in databases (Zuiderweg, 2002; Bairoch et al., 2005). Comparative modeling is widely recognized as a reliable method to generate a 3D model of a target protein from its primary structure (Tramontano and Morea, 2003; Moult, 2005). An essential requirement for this method is the identification of at least one experimentally solved 3D structure of a protein homolog that can be used as the template.

Solutions could only be reasonably computed for interactions between DpsA/DpsB, DpsA/DpsD, DpsAB/DpsD, DpsAB/DpsY, DpsD/DpsY, and DpsD/DpsE. An interaction between KS$\alpha$ (DpsA), KS$\beta$ (DpsB), and the ACP (DpsG) could not be predicted using a monomeric model of KS$\alpha$ (DpsA) and KS$\beta$ (DpsB). Identifying the residues involved in the crucial interaction between the ACP and KS subunits will be a matter of important future research that will require more sophisticated biophysical methods (e.g., electron microscopy). Both programs returned solutions for KS$\alpha$ (DpsA) and KS$\beta$ (DpsB) models that matched the predicted 2.0 Å X-ray crystal structure of the KS subunits from the actinorhodin-producing PKS (Figure 1). It was the first solution from FireDock and the second from ClusPro. The C$\alpha$ rmsd of superimposed solutions was 0.42 Å. Stroud and coworkers (Keatinge-Clay et al., 2003) reported that the two KS subunits interact via tight complementary contacts that bury over one-fifth of the surface area of each monomer, forming an amphipathic tunnel. The cavity at the interface of the two monomers is where the polyketide backbone is synthesized, and its 17.0 Å length influences the chain length of the growing polyketide (Keatinge-Clay et al., 2004). A "grasping loop" structure formed between the $\alpha$7 helix of the KS$\alpha$ and $\alpha$8 helix of the KS$\beta$ is responsible for the tight interactions between the two subunits. In particular, Tyr118 of KS$\alpha$ and the Phe116 of KS$\beta$, were found to be involved in establishing close interactions. The active sites of the KS$\alpha$, Cys169 and Phe116 are thought to represent the gating residues that regulate chain length marking the beginning and the end of the amphipathic tunnel, respectively (Keatinge-Clay et al., 2004). Tyr118 is conserved in the same position in the amino acid sequence of KS$\alpha$ (DpsA), whereas Phe116 of KS$\beta$ is substituted by leucine on position 118 (Leu118) in the model (position Leu138 in the primary sequence) of KS$\beta$ (DpsB). With the substitution of Phe with Leu, the length of the amphiphatic tunnel is increased to ~19 Å, possibly reflecting the difference in acyl chain length between actinorhodin and daunorubicin polyketides. In a similar fashion to the actinorhodin system, we can speculate, based on the docking simulation using the predicted 3D structures of KS$\alpha$ (DpsA) and KS$\beta$ (DpsB), that the aklanonic acid backbone is also synthesized in a polyketide tunnel, the length of which is determined by the distance between the two residues, Cys169 on DpsA and Leu118 on DpsB (Phe116 on act CLF). The docking simulation with two DpsA monomers revealed a complex that was comparable with the crystal structure of the actinohrodin KS-CLF complex and predicted DpsA-DpsB complex. This was the first solution from both docking methods. The C$\alpha$ rmsd of superimposed solutions was 1.92 Å.

The proposed orientation (Figure 1) for the interaction between DpsAB/DpsD showed that docking of DpsD occurs in a pocket on DpsA created between helices $\alpha$2 Pro57-Ala60, $\alpha$3 Ala64-Arg69, $\alpha$6 Thr111-Ser122, and the loop formed from residues Ser38-Arg46, which is located between helices $\alpha$1 and $\alpha$2. In this interaction, DpsD is involved with two $\alpha$ helices from small subunit $\alpha$8 (Gly149–Asn15) and $\alpha$9 (Val174–Leu184) and the N terminus of helix $\alpha$10 (Pro203-Thr219), from which Pro203 and Met204 are involved in establishing hydrophobic interactions

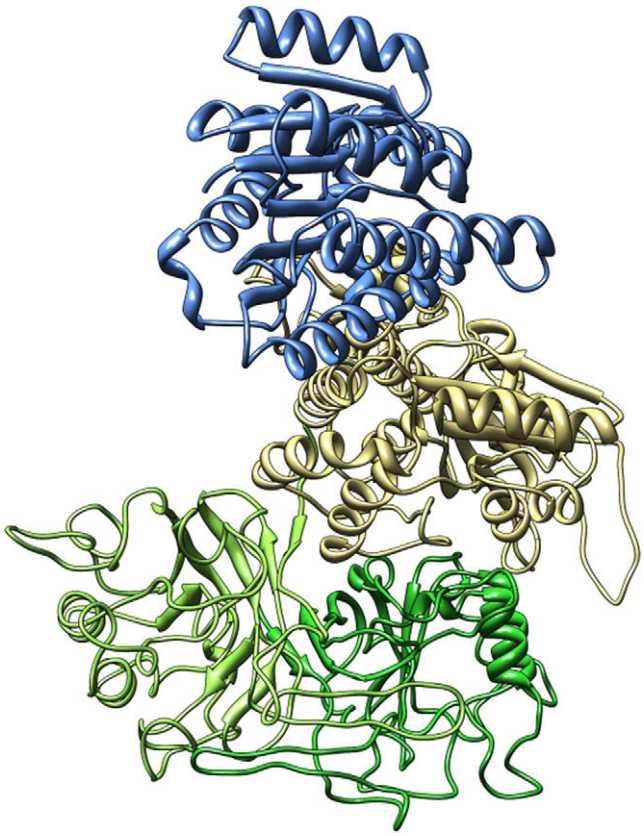

**Figure 2. Superimposed Computational Docking Solutions for the Protein-Protein Interactions between DpsD/DpsE and DpsY/DpsD**
DpsE (blue) docks in a region between the small subunit and helical flap of DpsD (yellow). The DpsY subunits (in different shades of green) interact planar to DpsD.

with Phe55 from the loop connecting helices 1 and 2 on DpsA. It is possible that flexible docking would show closer interactions with the conformational change in the loop connecting helices 1 and 2 in the DpsA. In the Y2H assays, KSα (DpsA) was found to establish homotypic interactions. In order to investigate whether this association would have any influence on the orientation of the interaction with MCAT (DpsD), a docking simulation was also performed between KSα (DpsA), as a homodimer, and MCAT (DpsD), and the DpsA monomer with DpsD. In both simulations, matching complexes were the first solutions from both programs.

The proposed orientation for the docking between MCAT (DpsD) and the homodimer of the CYC (DpsY) revealed an interesting interface between these two proteins (Figure 2). This was the eighth solution in Firedock and the third solution in ClusPro. The MCAT (DpsD) appeared to interact mainly via interactions established with the C terminus of helix α10 (Pro203–Ser218), the N terminus of helix α11 (Leu240–Leu252), and the loop connecting these helices (Thr219–Gln239). DpsY interacts with both of its subunits, with DpsD helix α10, penetrating into a pocket between the monomer subunits. The β1 sheet (Met6–Glu8) and loop connecting β sheets 2 and 3 from one DpsY monomer, and the loops connecting sheet β4 and helix α2, and sheet β6 and helix α3 from the second DpsY monomer are involved in the interaction.

The simulation for the docking between the MCAT and KR (DpsD/DpsE) revealed a particular interface chosen from the first solution of FireDock and the second of ClusPro with a Cα RMSD of 1.92 Å (Figure 2). MCAT (DpsD) takes part in the interaction with the helices α3 (Arg54–Asp60), α4 (Ala63–Asp67) and the loop connecting helices α2 and α3 (Asp40–Leu53). This corresponds to the region between the small subunit and helical flap of MCAT. The KR (DpsE) contributes to the interface with the C-terminal region of helix α8 (Glu205–Lys215), α6 (Ala150–Leu170), small helix α5 (Thr140–Gly142), and the loop connecting helices α5 and α6 (Lys143–Gly149). Hydrophobic amino acid residues are also likely to be involved in establishing the interaction. The simulation for the docking between the KS-CLF/CYC (DpsA-B/DpsY) showed an interesting complex where DpsY dimmer positions itself on DpsA in the proximity of the entrance to the amphipathic tunnel. The selected complex was the first solution in FireDock and the fifth in ClusPro. The DpsY dimer in this solution interacts with both KS and CLF. DpsY takes part in the interaction mostly with loops used in subunit binding that interact with helix α16 (Lys314–Tyr333), C terminal of helix α11 (Pro202–Ala210) and a loop connecting sheet β6 and helix α14 (Asn271–Gly282) on DpsA, and with helix α7 (Pro126–His128), helix α4 (Lys66–Gln71) and loop connecting helix α5 and sheet β4 (Ser90–Glu99) on DpsB. This arrangement of proteins would be favorable to reducing spontaneous cyclization, and is also in close proximity to the amphipathic tunnel (Figure 3). This represents what is, to our knowledge, the first study attempting to analyze in vivo protein interactions forming a type II PKS. A better understanding of the protein-protein interactions within the type II PKS complex should allow us to formulate new design rules for the synthesis of aromatic polyketides through combinatorial biosynthesis.

## SIGNIFICANCE

**Using a yeast two-hybrid (Y2H) screen, the core components forming the polyketide synthase (PKS) complex were the ketosynthase (KS) subunits, predicted to be a heterotetramer with the two KSα (DpsA) polypeptides interacting strongly with each other, and with KSβ (DpsB). The heterodimeric core was further extended to include two malonyl-CoA:ACP acyltransferase (MCAT) (DpsD) polypeptides, again interacting strongly with KSα (DpsA). Correlating our data with those of previous in vivo and in vitro experiments (Rajgarhia et al., 2001), we propose that, within the complex, the MCAT (DpsD) might act in a structural role; perhaps its physical position prevents chain initiation using an acetate starter. The cyclase (CYC) (DpsY) was found to interact with all of the proteins forming the complex, which may indicate a significant structural role, maintaining the complex in a biologically active configuration, as has been suggested for post-PKS modifying activities of other type II complexes (Petkovic et al., 1999; Perić-Concha et al., 2005). From the Y2H assays, KSα (DpsA) was predicted to play a key role in the proposed head-to-tail arrangement of the "minimal" PKS and, therefore, was chosen as the target protein to fuse to the tandem affinity purification tag. The "pulldown" experiments resulted in the purification of the KSα (DpsA) and KSβ (DpsB)**

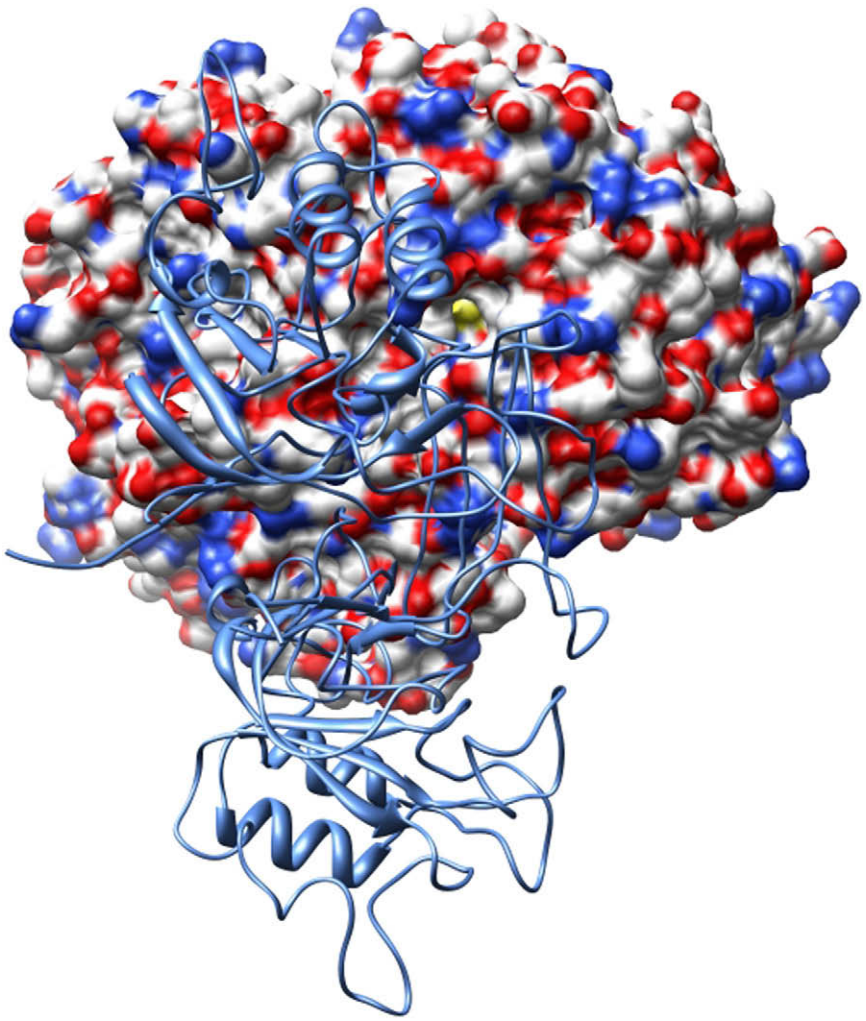

**Figure 3. Computational Docking Simulating the Protein-Protein Interactions between DpsAB and DpsY**

The location of the docking site is in the proximity of the entrance to the amphipathic tunnel (shown yellow on DpsAB surface). The entrance to the cavity containing active site of DpsY is also in the proximity of the entrance to the amphiphatic tunnel (Thompson et al., 2004). The surface of the DpsAB complex is colored based on hydrophobic properties of the residues using the Kyte-Doolittle scale. Colors range from blue, for the most hydrophilic residues, through white, and then to red for the most hydrophobic residues.

**subunits, but failed to copurify the MCAT (DpsD), which, from the previous Y2H results, was predicted to interact strongly with KSα (DpsA). Both programs used for docking simulations were also able to predict a docking orientation for KSα/KSβ (DpsA/DpsB), similar to that observed for the solved crystal structure of the actinorhodin KSα/KSβ heterodimer (Keatinge-Clay et al., 2004). The docking simulations also suggest that the MCAT (DpsD) might have a structural role in bringing the active sites of the ketoreductase (DpsE) and the CYC (DpsY) in to close proximity, allowing the proteins to carry out adjacent modifications of the aklanonic acid backbone in conjunction with the CYC/aromatase (DpsF).**

## EXPERIMENTAL PROCEDURES

### Y2H Experiments

Each *dps* gene was subcloned by PCR using the plasmid template pWHM1012. All the forward primers were designed incorporating an *Nde*I site upstream of the translational start codon, while all the reverse primers were designed with an EcoRI site downstream of the translational stop codon (Table S1). The amplified products were purified from agarose gels using QIAEX II following the manufacturer's instructions (QIAGEN GmbH, Hilden, Germany). The purified fragments were then cloned via NdeI/EcoRI recognition sites into the polylinker of both Y2H plasmids pGADT-7 (prey) and pGBKT-7 (bait). The constructs were sequenced to check that the *dps* gene inserts were in frame with Gal4-AD (pGADT-7) and Gal4-BD (pGBKT-7). Y2H experiments were performed in *S. cerevisiae* AH109 using procedures described by the manufacturer (BD Biosciences/Clonetech, Palo Alto, CA). Triplicate yeast transformations, using each *dps* gene in combination as both prey and bait, were plated out on both SD-2 (Trp- and Leu-) and SD-4 (Trp-, Leu-, Ade-, and His-) media and incubated at 30°C for up to 14 days. Colony lift *LacZ* assays were also performed on yeast cells grown on SD-2 medium to verify protein interactions. Protein expression was checked where no interactions were observed. Protein extraction was performed using 1 ml of SD-2 cultures ($1 \times 10^7$ cells $ml^{-1}$) with trichloroacetic acid. Precipitated proteins were resuspended in 300 μl of SU buffer (5% w/v SDS, 8 M urea, 125 mM Tris-HCl, pH 6.8, 0.1% EDTA, 15 mg/ml DTT, and 0.005% w/v bromophenol blue). The proteins were separated by 10% SDS-PAGE and electroblotted onto nitrocellulose membranes for Western blot analysis. The antibodies used to perform Western blots were obtained from Abcam Limited (Cambridge, UK). The primary antibodies were mouse monoclonal anti-c-Myc and mouse monoclonal anti-HA tag. The secondary antibody was a rabbit polyclonal to the mouse IgG H&L horseradish peroxidase-conjugated anti-IgG. Detection was performed using 3,3′,5,5′-tetramethylbenzidine, as specified by the manufacturer (Sigma Aldrich, St. Louis, MO).

### TAP

Plasmid designated pNC147 is a derivative of pWHM1012 encoding the genes *dpsA, dpsB, dpsC, dpsD*, nd *dpsG*, which translates a TAP tag fused to the N terminus of DpsA. Details of the cloning strategy to construct pNC147, in five steps, are described in Figure S2. Expression of proteins encoded by pNC147 used the heterologous host *S. coelicolor* A3(2) grown in 50 ml of YEME medium supplemented with thiostrepton (15 μg/ml) as described by Kieser et al. (2000). The mycelium was collected by centrifugation and washed twice with 0.09 M Tris-Cl, pH 7.9. The TAP tag procedure followed was as described by Rigaut et al. (1999). Proteins were separated by 1D SDS-PAGE and digested in-gel with trypsin. The peptide digests were extracted from each gel band and separated by nanoRP-LC (Micromass CapLC, Waters) before MS analysis using a Q-TOF Ultima Global (Waters). The mass spectrometric acquisition was performed in a data-dependent manner, with a 1 s MS survey scan followed by MS/MS scans (1 s) on the 3 most abundant multiply charged ions. The raw MS/MS spectra were processed to 'pkl' files using MassLynx software version 4.1 (Waters) and analyzed using GeneBio Phenyx Software (Geneva, Switzerland).

### Computer Docking Simulations

Two sets of models were built. One using Swiss-Model (Arnold et al., 2006; Guex and Peitsch, 1997) and the other using MODELER 9.4 (Fiser and Sali, 2003). Both sets were evaluated using DOPE function (Shen and Sali, 2006) from MODELER 9.4 and Verify3D (Mashiach et al., 2008). Models with the most favorable energy profile and profile score were selected for protein-protein docking simulations. For Swiss-Model 3D templates were chosen based on the results obtained using GenTHREADER (McGuffin et al., 2000), Modbase (McGuffin et al., 2000) and Predict protein (Rost et al., 2003). Templates used in MODELER were selected by scanning the query sequence against a library of sequences extracted from known structures in Protein Data Bank (PDB), which was obtained from MODELER (http://salilab.org/modeller/). Alignments were created with MODELER, unless stated otherwise. The DpsA model was built using the "Automated Mode" in Swiss-Model with 1TQYA as a template which has 62.5% sequence identity to DpsA. The DpsB model was built using the "Automated Mode" in Swiss-Model with 1TQYB as a template which has 57.75% sequence identity to DpsB. The DpsC model was built using the "Project Mode" in Swiss-Model with 1HNJA as the template which had 22.3% sequence identity to DpsC. The model was built based on an mGenTHREADER (McGuffin et al., 2000) sequence alignment and optimized using the SWISS-MODEL server (Arnold et al., 2006). The DpsD model was built using MODELER 9.4. As templates, 1MLAA (30% identity), 1NM2A (34% identity) and 2CUYA (32% identity) were used. The DpsE model was built using MODELER 9.4; 1X7GA (59% identity) and 2PH3A (41% identity) were used as templates. The DpsF model was built using MODELER 9.4 with 2RERA as the template, which had 23.2% sequence identity to DpsF. The model was built based on an mGenTHREADER sequence alignment. The DpsG model was built using MODELER 9.4; 1NQ4A (40% identity), 1OR5A (38% identity), and 1AF8A (38% identity) were used as templates. The DpsY model was built using MODELER 9.4 with 1R61A as the template, which had 24.9% sequence identity to DpsY. The model was built based on an mGenTHREADER sequence alignment; the model was built as a dimer. Sequence alignments are available upon request to the corresponding author.

These proposed models cover the KS$\alpha$ (DpsA) amino acid sequence from Arg3 to Arg419, with the expected structural characteristics including the position of the catalytic Cys169. The model for KS$\beta$ covers amino acid sequence from Arg26 to Ala424, with the highly conserved Gln161 of the actinorhodin homolog occupying position 183 in the primary sequence of KS$\beta$ (DpsB). The homodimer of KS$\alpha$ (DpsA) was obtained by docking simulation using PatchDock/FireDock. The heterodimer of DpsA/DpsB was obtained by docking simulation using PatchDock/FireDock (first solution). The putative models for the MCAT (DpsD) and KR (DpsE) cover their entire primary structure. A 3D structure for the CYC (DpsY) was modeled using the deposited structure of a predicted metal-dependent hydrolase from *Bacillus stearothermophilus* as a template (PDB accession code: 1R61). This template was chosen based on mGENthreader results. The model for the CYC (DpsY) covers its amino acid sequence from Thr12 to Glu272. Protein docking simulations between each pair of predicted 3D structures were performed using PatchDock and ClusPro. PatchDock was used with default settings and the best 100 solutions were refined using FireDock. The first 10 solutions were returned as results. ClusPro was used with default settings, and ZDOCK was used as the docking program. The top 10 solutions were returned as results. Solutions that were found by both programs were chosen for analysis of the interface. Docking simulation between the two KS subunits (DpsA and DpsB) were performed using KS$\alpha$ (DpsA) as receptor and KS$\beta$ (DpsB) as ligand, based upon the published crystal structure for the actinorhodin orthologs. Docking simulation between KS$\alpha$/CYC (DpsA/DpsY) were performed using the dimer of the CYC (DpsY) as receptor and KS$\alpha$ (DpsA) as ligand. A docking simulation between KS$\beta$ and CYC (DpsB/DpsY) was performed in a similar fashion. The docking between the two subunits of the KS dimer (DpsA/DpsB) and the homodimer of the CYC (DpsY) was performed using the KS$\alpha$/KS$\beta$ (DpsA/DpsB) dimer as receptor and the CYC (DpsY) homodimer as ligand. Docking simulation between the KS$\alpha$ and MCAT (DpsA/DpsD) was performed using KS$\alpha$ (DpsA) as receptor and MCAT (DpsD) as ligand. Docking between homodimer of KS$\alpha$ (DpsA) and MCAT (DpsD) was also performed using the KS$\alpha$ (DpsA) homodimer as receptor and MCAT (DpsD) as ligand. For the KR/CYC (DpsE/DpsY) simulation, the homodimer of the CYC (DpsY) was the receptor and KR (DpsE) was the ligand. The MCAT/CYC (DpsD/DpsY) docking was simulated using the homodimer of the CYC (DpsY) as receptor and MCAT (DpsD) as ligand. The MCAT/KR (DpsD/DpsE) docking was simulated using MCAT (DpsD) as receptor and KR (DpsE) as ligand.

## SUPPLEMENTAL DATA

Supplemental Data include one table and seven figures and can be found with this article online at http://www.chembiol.com/cgi/content/full/15/11/1156/DC1/.

## ACKNOWLEDGMENTS

This work was supported by Wellcome Trust grant 064197 to P.F.L., the Central Research Fund, University of London (ref: AR/CRF/B), by Ministry of Science, Education, and Sports, Republic of Croatia grant TP-05/0058-23 to D.H. and J.Z., and by a stipend from the School of Pharmacy, University of London, to G.C. and S.H. The authors would like to thank M. Smith and F.A. Stephenson for their technical support and advice.

Received: March 28, 2008
Revised: August 9, 2008
Accepted: September 4, 2008
Published: November 21, 2008

## REFERENCES

Andrusier, N., Nussinov, R., and Wolfson, H.J. (2007). FireDock: fast interaction refinement in molecular docking. Proteins *69*, 139–159.

Arnold, K., Bordoli, L., Kopp, J., and Schwede, T. (2006). The SWISS-MODEL Workspace: A web-based environment for protein structure homology modelling. Bioinformatics *22*, 195–201.

Bairoch, A., Apweiler, R., Wu, C.H., Barker, W.C., Boeckmann, B., Ferro, S., Gasteiger, E., Huang, H., Lopez, R., Magrane, M., et al. (2005). The Universal Protein Resource (UniProt). Nucleic Acids Res. *33*, D154–D159.

Bao, W., Sheldon, P.J., and Hutchinson, C.R. (1999a). Purification and properties of the *Streptomyces peucetius* DpsC beta-ketoacyl:acyl carrier protein synthase III that specifies the propionate-starter unit for type II polyketide biosynthesis. Biochemistry *38*, 9752–9757.

Bao, W., Sheldon, P.J., Wendt-Pienkowski, E., and Hutchinson, C.R. (1999b). The *Streptomyces peucetius* dpsC gene determines the choice of starter unit in biosynthesis of the daunorubicin polyketide. J. Bacteriol. *181*, 4690–4695.

Beinker, P., Lohkamp, B., Peltonen, T., Niemi, J., Mantsala, P., and Schneider, G. (2006). Crystal structures of SnoaL2 and AclR: two putative hydroxylases in the biosynthesis of aromatic polyketide antibiotics. J. Mol. Biol. *359*, 728–740.

Bibb, M.J., Sherman, D.H., Omura, S., and Hopwood, D.A. (1994). Cloning, sequencing and deduced functions of a cluster of *Streptomyces* genes probably encoding biosynthesis of the polyketide antibiotic frenolicin. Gene *142*, 31–39.

Bisang, C., Long, P.F., Cortés, J., Westcott, J., Crosby, J., Matharu, A.-L., Cox, R.J., Simpson, T.J., Staunton, J., and Leadlay, P.F. (1999). A chain initiation factor common to both aromatic and modular polyketide synthases. Nature *401*, 502–505.

Carreras, C.W., and Khosla, C. (1998). Purification and *in vitro* reconstitution of the essential protein components of an aromatic polyketide synthase. Biochemistry *37*, 2084–2088.

Castaldo, G., Crosby, J., and Long, P.F. (2005). Exploring protein interactions on a minimal type II polyketide synthase using a yeast two-hybrid system. Food Technol. Biotechnol. *43*, 109–112.

Chen, R., Li, L., and Weng, Z. (2003). ZDOCK: an initial-stage protein-docking algorithm. Proteins *52*, 80–87.

Comeau, S.R., Gatchell, D.W., Vajda, S., and Camacho, C.J. (2003). ClusPro: an automated docking and discrimination method for the prediction of protein complexes. Bioinformatics *20*, 45–50.

Crump, M.P., Crosby, J., Dempsey, C.E., Parkinson, J.A., Murray, M., Hopwood, D.A., and Simpson, T.J. (1997). Solution structure of the actinorhodin

polyketide synthase acyl carrier protein from *Streptomyces coelicolor* A3(2). Biochemistry *36*, 6000–6008.

Decker, H., Summers, R.G., and Hutchinson, C.R. (1994). Overproduction of the acyl carrier protein component of a type II polyketide synthase stimulates production of tetracenomycin biosynthetic intermediates in *Streptomyces glaucescens*. J. Antibiot. (Tokyo) *47*, 54–63.

Dreier, J., and Khosla, C. (2000). Mechanistic analysis of a type II polyketide synthase. Role of conserved residues in the beta-ketoacyl synthase-chain length factor heterodimer. Biochemistry *39*, 2088–2095.

Duhovny, D., Nussinov, R., and Wolfson, H.J. (2002). Efficient unbound docking of rigid molecules. In Proceedings of the 2nd Workshop on Algorithms in Bioinformatics (WABI), R. Guigo and D. Gusfield, eds. (New York: Springer), 185–200.

Findlow, S.C., Winsor, C., Simpson, T.J., Crosby, J., and Crump, M.P. (2003). Solution structure and dynamics of oxytetracycline polyketide synthase acyl carrier protein from *Streptomyces rimosus*. Biochemistry *42*, 8423–8433.

Fiser, A., and Sali, A. (2003). Comparative protein structure modeling with MODELLER: a practical approach. Methods Enzymol. *374*, 463–493.

Florova, G., Kazanina, G., and Reynolds, K.A. (2002). Enzymes involved in fatty acid and polyketide biosynthesis in *Streptomyces glaucescens*: role of FabH and FabD and their acyl carrier protein specificity. Biochemistry *41*, 10462–10471.

Funa, N., Ohnishi, Y., Fujii, I., Shibuya, M., Ebizuka, Y., and Horinouchi, S. (1999). A new pathway for polyketide synthesis in microorganisms. Nature *400*, 897–899.

Gramajo, H.C., White, J., Hutchinson, C.R., and Bibb, M.J. (1991). Overproduction and localization of components of the polyketide synthase of *Streptomyces glaucescens* involved in the production of the antibiotic tetracenomycin C. J. Bacteriol. *173*, 6475–6483.

Grimm, A., Madduri, K., Ali, A., and Hutchinson, C.R. (1994). Characterization of the *Streptomyces peucetius* ATCC 29050 genes encoding doxorubicin polyketide synthase. Gene *151*, 1–10.

Guex, N., and Peitsch, M.C. (1997). SWISS-MODEL and the Swiss-PdbViewer: an environment for comparative protein modelling. Electrophoresis *18*, 2714–2723.

Hadfield, A.T., Limpkin, C., Teartasin, W., Simpson, T., Crosby, J., and Crump, M.P. (2004). The crystal structure of the actIII actinorhodin polyketide reductase: proposed mechanism for ACP and polyketide binding. Structure *12*, 1865–1875.

Hertweck, C., Luzhetskyy, A., Rebets, Y., and Bechtold, A. (2007). Type II polyketide synthases: gaining a deeper insight into enzymatic teamwork. Nat. Prod. Rep. *24*, 162–190.

Hesketh, A.R., Chandra, G., Shaw, A.D., Rowland, J.J., Kell, D.B., Bibb, M.J., and Chater, K.F. (2002). Primary and secondary metabolism, and post-translational protein modifications, as portrayed by proteomic analysis of *Streptomyces coelicolor*. Mol. Microbiol. *46*, 917–932.

Hitchman, T.S., Crosby, J., Byrom, K.J., Cox, R.J., and Simpson, T.J. (1998). Catalytic self-acylation of type II polyketide synthase acyl carrier proteins. Chem. Biol. *5*, 35–47.

Hutchinson, C.R., and Colombo, A.L. (1999). Genetic engineering of doxorubicin production in *Streptomyces peucetius*: a review. J. Ind. Microbiol. Biotechnol. *23*, 647–652.

Jackowski, S., Murphy, C.M., Cronan, J.E., Jr., and Rock, C.O. (1989). Acetoacetyl-acyl carrier protein synthase. A target for the antibiotic thiolactomycin. J. Biol. Chem. *264*, 7624–7629.

Jansson, A., Koskiniemi, H., Mäntsälä, P., Niemi, J., and Schneider, G. (2004). Crystal structure of a ternary complex of DnrK, a methyltransferase in daunorubicin biosynthesis, with bound products. J. Biol. Chem. *279*, 41149–41156.

Kealey, J.T., Liu, L., Santi, D.V., Betlach, M.C., and Barr, P.J. (1998). Production of a polyketide natural product in nonpolyketide-producing prokaryotic and eukaryotic hosts. Proc. Natl. Acad. Sci. USA *95*, 505–509.

Keatinge-Clay, A.T., Shelat, A.A., Savage, D.F., Tsai, S.C., Miercke, L.J., O'Connell, J.D., Khosla, C., and Stroud, R.M. (2003). Catalysis, specificity, and ACP docking site of *Streptomyces coelicolor* malonyl-CoA:ACP transacylase. Structure *11*, 147–154.

Keatinge-Clay, A.T., Maltby, D.A., Medzihradszky, K.F., Khosla, C., and Stroud, R.M. (2004). An antibiotic factory caught in action. Nat. Struct. Mol. Biol. *11*, 888–893.

Kieser, T., Bibb, M.J., Buttner, M.J., and Hopwood, D.A. (2000). Practical *Streptomyces* Genetics (Norwich, UK: The John Innes Foundation).

Korman, T.P., Hill, J.A., Vu, T.N., and Tsai, S.C. (2004). Structural analysis of actinorhodin polyketide ketoreductase: cofactor binding and substrate specificity. Biochemistry *43*, 14529–14538.

Kramer, P.J., Zawada, R.J.X., McDaniel, R., Hutchinson, C.R., Hopwood, D.A., and Khosla, C. (1997). Rational design and engineered biosynthesis of a novel 18-carbon aromatic polyketide. J. Am. Chem. Soc. *119*, 635–639.

Li, Q., Khosla, C., Puglisi, J.D., and Liu, C.W. (2003). Solution structure and backbone dynamics of the holo form of the frenolicin acyl carrier protein. Biochemistry *42*, 4648–4657.

Lomovskaya, N., Doi-Katayama, Y., Filippini, S., Nastro, C., Fonstein, L., Gallo, M., Colombo, A.L., and Hutchinson, C.R. (1998). The *Streptomyces peucetius dpsY* and *dnrX* genes govern early and late steps of daunorubicin and doxorubicin biosynthesis. J. Bacteriol. *180*, 2379–2386.

Mashiach, E., Schneidman-Duhovny, D., Andrusier, N., Nussinov, R., and Wolfson, H.J. (2008). FireDock: a Web server for fast interaction refinement in molecular docking. Nucleic Acids Res. *36*, W229–W232.

Matharu, A.L., Cox, R.J., Crosby, J., Byrom, K.J., and Simpson, T.J. (1998). MCAT is not required for in vitro polyketide synthesis in a minimal actinorhodin polyketide synthase from *Streptomyces coelicolor*. Chem. Biol. *5*, 699–711.

McDaniel, R., Ebert-Khosla, S., Hopwood, D.A., and Khosla, C. (1995). Rational design of aromatic polyketide natural products by recombinant assembly of enzymatic subunits. Nature *375*, 549–554.

McGuffin, L.J., Bryson, K., and Jones, D. (2000). The PSIPRED protein structure prediction server. Bioinformatics *16*, 404–405.

Meurer, G., Gerlitz, M., Wendt-Pienkowski, E., Vining, L.C., Rohr, J., and Hutchinson, C.R. (1997). Iterative type II polyketide synthases, cyclases and ketoreductases exhibit context-dependent behavior in the biosynthesis of linear and angular decapolyketides. Chem. Biol. *4*, 433–443.

Minotti, G., Menna, P., Salvatorelli, E., Cairo, G., and Gianni, L. (2004). Anthracyclines: molecular advances and pharmacologic developments in antitumor activity and cardiotoxicity. Pharmacol. Rev. *56*, 185–229.

Mootz, H.D., Finking, R., and Marahiel, M.A. (2001). 4′-phosphopantetheine transfer in primary and secondary metabolism of *Bacillus subtilis*. J. Biol. Chem. *276*, 37289–37298.

Moult, J. (2005). A decade of CASP: progress, bottlenecks and prognosis in protein structure prediction. Curr. Opin. Struct. Biol. *15*, 285–289.

Pan, H., Tsai, S., Meadows, E.S., Miercke, L.J., Keatinge-Clay, A.T., O'Connell, J., Khosla, C., and Stroud, R.M. (2002). Crystal structure of the priming beta-ketosynthase from the R1128 polyketide biosynthetic pathway. Structure *10*, 1559–1568.

Parrish, J.R., Gulyas, K.D., and Finley, R.L., Jr. (2006). Yeast two-hybrid contributions to interactome mapping. Curr. Opin. Biotechnol. *17*, 387–393.

Perić-Concha, N., Borovička, B., Long, P.F., Hranueli, D., Waterman, P.G., and Hunter, I.S. (2005). Ablation of the *otc*C gene encoding a post-polyketide hydroxylase from the oxytetracyline biosynthetic pathway in *Streptomyces rimosus* results in novel polyketides with altered chain length. J. Biol. Chem. *280*, 37455–37460.

Petkovic, H., Thamchaipenet, A., Zhou, L.H., Hranueli, D., Raspor, P., Waterman, P.G., and Hunter, I.S. (1999). Disruption of the aromatase/cyclase from the oxytetracycline gene cluster of *Streptomyces rimosus* results in production of novel polyketides with shorter chain lengths. J. Biol. Chem. *274*, 32829–32834.

Piel, J., Hertweck, C., Shipley, P.R., Hunt, D.M., Newman, M.S., and Moore, B.S. (2000). Cloning, sequencing and analysis of the enterocin biosynthesis gene cluster from the marine isolate '*Streptomyces maritimus*': evidence for the derailment of an aromatic polyketide synthase. Chem. Biol. *7*, 943–955.

Qin, J., Vinogradova, O., and Gronenborn, A.M. (2001). Protein-protein interactions probed by nuclear magnetic resonance spectroscopy. Methods Enzymol. *339*, 377–389.

Qiu, X., Janson, C.A., Smith, W.W., Head, M., Lonsdale, J., and Konstantinidis, A.K. (2001). Refined structures of β-ketoacyl-acyl carrier protein synthase III. J. Mol. Biol. *307*, 341–356.

Rajgarhia, V.B., and Strohl, W.R. (1997). Minimal *Streptomyces* sp. strain C5 daunorubicin polyketide biosynthesis genes required for aklanonic acid biosynthesis. J. Bacteriol. *179*, 2690–2696.

Rajgarhia, V.B., Priestley, N.D., and Strohl, W.R. (2001). The product of dpsC confers starter unit fidelity upon the daunorubicin polyketide synthase of *Streptomyces* sp. strain C5. Metab. Eng. *3*, 49–63.

Raty, K., Kantola, J., Hautala, A., Hakala, J., Ylihonko, K., and Mantsala, P. (2002). Cloning and characterization of *Streptomyces galilaeus* aclacinomycins polyketide synthase (PKS) cluster. Gene *293*, 115–122.

Revill, W.P., Bibb, M.J., and Hopwood, D.A. (1995). Purification of a malonyltransferase from *Streptomyces coelicolor* A3(2) and analysis of its genetic determinant. J. Bacteriol. *177*, 3946–3952.

Rigaut, G., Shevchenko, A., Rutz, B., Wilm, M., Mann, M., and Séraphin, B. (1999). A generic protein purification method for protein complex characterization and proteome exploration. Nat. Biotechnol. *17*, 1030–1032.

Rost, B., Yachdav, G., and Liu, J. (2003). The PredictProtein server. Nucleic Acids Res. *32*, W321–W326. 10.1093/nar/gkh377.

Schneidman-Duhovny, D., Inbar, Y., Nussinov, R., and Wolfson, H.J. (2005). PatchDock and SymmDock: servers for rigid and symmetric docking. Nucleic Acids Res. *33*, W363–W367. 10.1093/nar/gki481.

Shen, M.Y., and Sali, A. (2006). Statistical potential for assessment and prediction of protein structures. Protein Sci. *15*, 2507–2524.

Sultana, A., Kallio, P., Jansson, A., Wang, J.S., Niemi, J., Mäntsälä, P., and Schneider, G. (2004). Structure of the polyketide cyclase *SnoaL* reveals a novel mechanism for enzymatic aldol condensation. EMBO J. *23*, 1911–1921.

Summers, R.G., Ali, A., Shen, B., Wessel, W.A., and Hutchinson, C.R. (1995). Malonyl-coenzyme A: acyl carrier protein acyltransferase of *Streptomyces glaucescens*: A possible link between fatty acid and polyketide biosynthesis. Biochemistry *34*, 9389–9402.

Tang, Y., Lee, T.S., Kobayashi, S., and Khosla, C. (2003). Ketosynthases in the initiation and elongation modules of aromatic polyketide synthases have orthogonal acyl carrier protein specificity. Biochemistry *42*, 6588–6595.

Tang, Y., Lee, T.S., and Khosla, C. (2004). Engineered biosynthesis of regioselectively modified aromatic polyketides using bimodular polyketide synthases. PLoS Biol. *2*, E31. 10.1371/journal.pbio.0020031.

Thompson, T.B., Katayama, K., Watanabe, K., Hutchinson, C.R., and Rayment, I. (2004). Structural and functional analysis of tetracenomycin F 2 cyclase from *Streptomyces glaucescens*: a type II polyketide cyclase. J. Biol. Chem. *279*, 37956–37963.

Tramontano, A., and Morea, V. (2003). Assessment of homology-based predictions in CASP5. Proteins *53*, 352–368.

Wattanachaisaereekul, S., Lantz, A.E., Nielsen, M.L., and Nielsen, J. (2008). Production of the polyketide 6-MSA in yeast engineered for increased malonyl-CoA supply. Metab. Eng. Epub ahead of print May 10, 2008. 10.1016/j.ymben.2008.04.005.

White, S.W., Zheng, J., Zhang, Y.M., and Rock, C.O. (2005). The structural biology of type II fatty acid biosynthesis. Annu. Rev. Biochem. *74*, 791–831.

Wohlert, S.E., Wendt-Pienkowski, E., Bao, W., and Hutchinson, C.R. (2001). Production of aromatic minimal polyketides by the daunorubicin polyketide synthase genes reveals the incompatibility of the heterologous DpsY and JadI cyclases. J. Nat. Prod. *64*, 1077–1080.

Yu, T.-W., Shen, Y., McDaniel, R., Floss, H.G., Khosla, C., Hopwood, D.A., and Moore, B.S. (1998). Engineered biosynthesis of novel polyketides from *Streptomyces* spore pigment polyketide synthases. J. Am. Chem. Soc. *120*, 7749–7759.

Zuiderweg, E.R. (2002). Mapping protein-protein interactions in solution by NMR spectroscopy. Biochemistry *41*, 1–7.